Am J Cancer Res 2023;13(7):2984-2997
www.ajcr.us /ISSN:2156-6976/ajcr0149673

Original Article

Development and validation of a N6 methylation regulator-related gene signature for prognostic and immune response prediction in non-small cell lung cancer

Xiang Li[1,2], Jinlong Ma[1,2], Zhenqian Sun[1,2], Na Li[3], Guangjun Jiao[1,2], Tianqi Zhang[4], Hongxin Cao[5,6]

[1]Qilu Hospital of Shandong University, Jinan 250000, Shandong, China; [2]Cheeloo College of Medicine, Shandong University, Jinan 250000, Shandong, China; [3]Mechanics Laboratory, Binzhou Medical University, Yantai 250000, Shandong, China; [4]Qilu Medical University, Zibo 250000, Shandong, China; [5]Department of Medical Oncology, Qilu Hospital of Shandong University, Jinan 250000, Shandong, China; [6]Key Laboratory of Chemical Biology (Ministry of Education), Institute of Biochemical and Biotechnological Drug, School of Pharmaceutical Sciences, Cheeloo College of Medicine, Shandong University, Jinan 250000, Shandong, China

Received February 15, 2023; Accepted June 20, 2023; Epub July 15, 2023; Published July 30, 2023

Abstract: N6 methylation (m6A) has been reported to play an important role in tumor progression. Non-small cell lung cancer (NSCLC) is the predominant pathological type of lung cancer with a high mortality rate. The purpose of this study was to develop and validate a N6 methylation regulator-related gene signature for assessing prognosis and response to immunotherapy in NSCLC. Data from The Cancer Genome Atlas was used as the training cohort. Data from Gene Expression Omnibus and Xena served as the two validation cohorts. We performed Cox regression, last absolute shrinkage and selection operator, receiver operating characteristic curves and Kaplan-Meier survival analysis to generate and validate a prognostic signature based on m6A regulator-related genes. We explored the association between the signature and tumor microenvironment including genomic mutation, immune cell infiltration and tumor mutation burden. We also analyzed the association between the signature and immunotherapy. Finally, among the genes that constituted the signature, GGA2 was the only favorable factor for NSCLC prognosis. Molecular experiments were used to explore GGA2 function in NSCLC. We generated a prognostic signature based on seven m6A regulator-related genes (GGA2, CD70, BMP2, GPX8, YWHAZ, NOG and TEAD4). And the data from three cohorts showed that the signature could effectively assess prognosis in NSCLC. Patients with high risk scores had the higher mutational load and lower immune infiltration levels and were more likely to not respond to immunotherapy. The experiments revealed overexpression of GGA2 inhibited proliferation and motility of NSCLC cells. Mechanically, GGA2 downregulated METTL3 expression and thus reduced m6A abundance in NSCLC. This study developed and validated a prognostic signature based on m6A regulator-related genes, providing useful insights for the management of NSCLC. And GGA2 may be a target of m6A regulation.

Keywords: N6 methylation, non-small cell lung cancer, prognostic signature, immunotherapy response, GGA2

Introduction

In the last decade, N6 methylation (m6A) of adenosine has been the most commonly observed reversible mRNA modification in eukaryotes [1, 2]. Unlike DNA methylation and histone modifications, RNA modifications have recently been highlighted as a new dimension of epigenetic regulation at the posttranscriptional RNA level [3]. All m6A modifications are strictly sequence specific, do not require extended sequences or secondary structures, and occur in only a small fraction of transcripts [4].

M6A is catalyzed by the methyltransferase complex, which consists of the writer proteins METTL3, METTL14 and WTAP. Its demethylation is catalyzed by two “eraser” demethylases, FTO and ALKBH5 [5-7]. YTHDF1, YTHDF2, YTHDF3, YTHDC1 and NHRNPA2B1, which are members of the YTH structural domain protein

family, are the m6A "readers" that recognize their modifications and influence pre-mRNA splicing as well as mRNA transport, stability and translation [8, 9]. Writers can colocalize with mammalian RNA methylation through m6A deposition [10]. Erasers apply as a reversible internal modification that catalyzes m6A demethylation [11]. In the cytoplasm of eukaryotes, the reader selectively binds m6A-containing mRNAs [12]. To date, more than 12,000 m6A sites in the transcripts of over 7,000 mammalian genes have been characterized by immunoprecipitation sequencing of methylated RNA [13]. Thus, RNA modifications play a crucial role in important biological processes in mammals.

Recently, several studies have shown that alterations in core genes during m6A modifications affect tumorigenesis and proliferation, the tumor microenvironment and prognosis [14, 15]. Genetic alterations and epigenetic modifications are also increasingly recognized as important regulators of cancers. However, there has been little progress in understanding the biological functions and mechanisms underlying the actions of m6A in non-small cell lung cancer (NSCLC) [16].

To gain further insight into the role of m6A in tumors, we investigated the relationship between NSCLC and m6A regulator-related genes. The results showed that alterations in the m6A regulator-related genes led to significant changes in the overall survival (OS) of patients with NSCLC. In brief, the identification of m6A-associated risk factors in NSCLC can help in the development of targeted therapy, early detection and treatment strategies for tumors.

Materials and methods

Data collection and processing

This study involved datasets from The Cancer Genome Atlas (TCGA), which including transcriptome data, mutation data and copy number variation (CNV) data. The count data were analyzed after log2 processing. We calculated the number of mutated genes in each sample.

For the validation cohorts, we collected the expression profile and clinical characteristics from NSCLC patients that were published by GSE81089 and Raponi 2006. GSE81089 was downloaded from the Gene Expression Omnibus (GEO). Raponi 2006 lung cancer data were downloaded from Xena.

Acquisition of m6A regulator-related genes and enrichment analysis

A total of 21 m6A regulators were identified according to a previous study [17]. These 21 m6A regulators included 8 writers (METTL3, METTL14, RBM15, RBM15B, WTAP, KIAA1429, CBLL1, ZC3H13), 2 erasers (ALKBH5, FTO) and 11 readers (YTHDC1, YTHDC2, YTHDF1, YTHDF2, YTHDF3, IGF2BP1, HNRNPA2B1, HNRNPC, FMR1, LRPPRC, ELAVL1). The expression of m6A regulators were entered into the downstream analysis after Z score conversion.

We performed the Pearson test to analyze the data regarding gene expression, CNV and number of mutations. Then, the correlation coefficients between the m6A regulator and other genes in each sample were obtained. Furthermore, genes that were significantly correlated with each m6A regulator in all three terms were identified using the absolute value of the correlation coefficient ≥ 0.2 and $P < 0.05$ as screening conditions.

The 'clusterProfiler' R package was used for enrichment analysis of the identified genes in Gene Ontology (GO) and Kyoto Encyclopedia of Genes and Genomes (KEGG). In addition, we used 'ClueGO' and 'BinGo' in Cytoscape software to analyze and visualize the network interactions between KEGG pathways and GO network interactions, respectively.

Construction and validation of the prognostic gene signature

Univariate Cox regression was used to screen for prognosis-related genes from the m6A regulator-related genes. Then, the last absolute shrinkage and selection operator (LASSO) was used for further screening and generation of risk scores.

In the training cohort, all samples were divided into high-risk and low-risk groups based on the median risk score. The predictive power of the risk scores was assessed using receiver operating characteristic (ROC) curves and Kaplan-Meier (KM) survival analysis. These analyses

were repeated in the validation cohorts. To further assess the validity and stability of the signature, we extracted clinical characteristics from the TCGA datasets for subgroup stratification analysis.

Analysis of tumor environment and immunotherapy response

To elucidate the genomic differences between the two groups, we analyzed the mutations. Next, we analyzed immune infiltration levels in the two groups using Cibersort. Finally, we explored the correlation between the risk score and the tumor stemness index, tumor microenvironment (TME) scores and tumor mutation burden (TMB) using the Spearman test.

We used the IMvigor210CoreBiologies dataset to investigate whether the risk score could be used as a marker of immunotherapy response. And we detected the difference in risk score between non-responders and responders. In addition, the proportion of non-responders in the high-risk and low-risk groups was also calculated.

Cell transfection and human tissue collection

Among the genes that constituted the signature, GGA2 was the only protective factor for prognosis (hazard ratio < 1). Therefore, a series of experiments was performed to explore its role in NSCLC.

Three NSCLC cell lines (A549, H1299 and H520) were involved in this study. All cell lines were purchased from Procell Biotechnology Co., Ltd. (Wuhan, China) and cultured according to the instructions.

GGA2 overexpression plasmid were purchased from Genechem (Shanghai, China). Small interference RNA (siRNA) of GGA2 negative control siRNA (siNC) were purchased from Genepharma (Shanghai, China). Cells were transfected according to the manufacturer's instructions. We used PCR to analyze transfection efficiency.

Tumor and its paired normal tissues were collected from patients who underwent surgery for NSCLC in our institution. Each sample was diagnosed independently by two pathologists.

Western blot analysis and PCR

Total proteins were extracted from cells using RIPA buffer (Cell Signaling Technology, Danvers, MA, USA). Western blot was performed according to previous study [18]. Antibodies used were: METTL3 (1:1000), METTL14 (1:1000), WTAP (1:1000), FTO (1:1000), ALKBH5 (1:1000). B-actin (1:1000) was set as control. All antibodies were purchased from Cell Signaling Technology.

Total RNA was extracted from cells and tissues using TRIzol reagent (Life Technologies, CA, USA). PCR was performed to detect mRNA expression levels according to previous study [19]. B-actin was set as control and relative mRNA expression levels were calculated by the $2^{-\Delta\Delta Ct}$ method. The sequences of primers were included in Supplementary Table 1.

Detecting the role of GGA2 in NSCLC cells

Cells were seeded at a density of 1×10^3 cells/well in 96-well plate for CCK-8 assays. At specific timepoints, 10 μl of CCK-8 reagent was added. After incubation at 37°C for 60 minutes, optical density (OD) was measured at 450 nm.

The fraction of DNA-replicating cells, which represented cell proliferation status, was assessed using EdU Detection Kit (RiboBio, Guangzhou, China).

Transwell assays were performed according to previous study [20]. At the beginning, 1×10^4 cells per group were inoculated in the upper chamber.

The m6A% content in total RNA was detected by MethyFlash m6A DNA Methylation ELISA Kit (Colorimetric) (A&D Technology Corporation, Beijing, China).

Statistical analysis and ethics statement

All experiments were carried out at least three independent times. Continuous variable was expressed as mean and standard deviation. Group differences for continuous variables were investigated with 2-tailed Student t test or Wilcoxon-Mann-Whitney nonparametric tests (2-tailed). Statistical significance was set at $P < 0.05$. All analyses were performed in R (version 4.1.2).

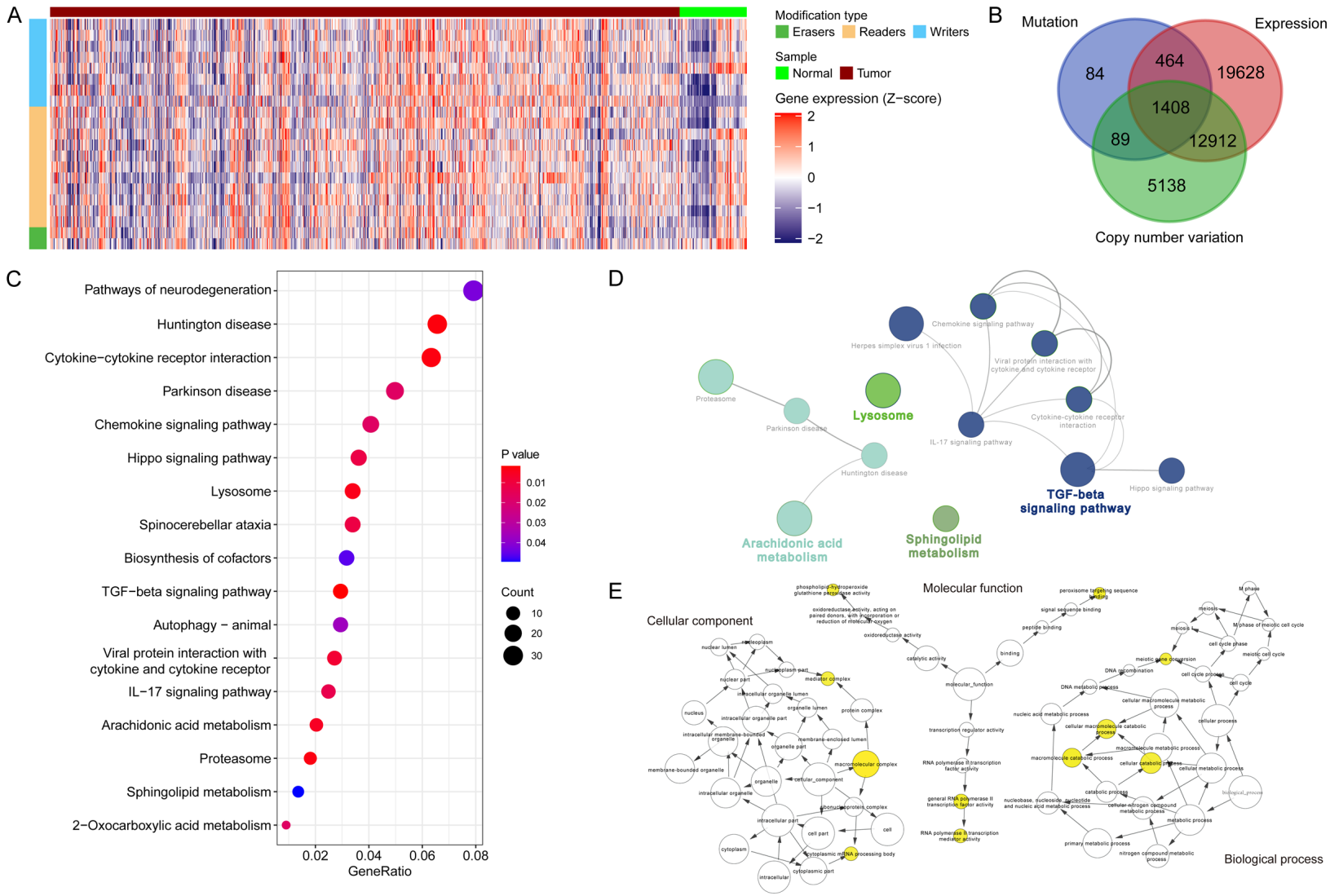

Figure 1. Acquisition of the genes significantly associated with m6A regulators and functional enrichment analysis. Differential expression of m6A regulators between tumor samples (n = 1015) and normal samples (n = 108) (A). The intersection of mutation, expression and copy number variation (B). Enriched signaling pathways in KEGG (C). Interaction network analysis in KEGG (D) and GO (E).

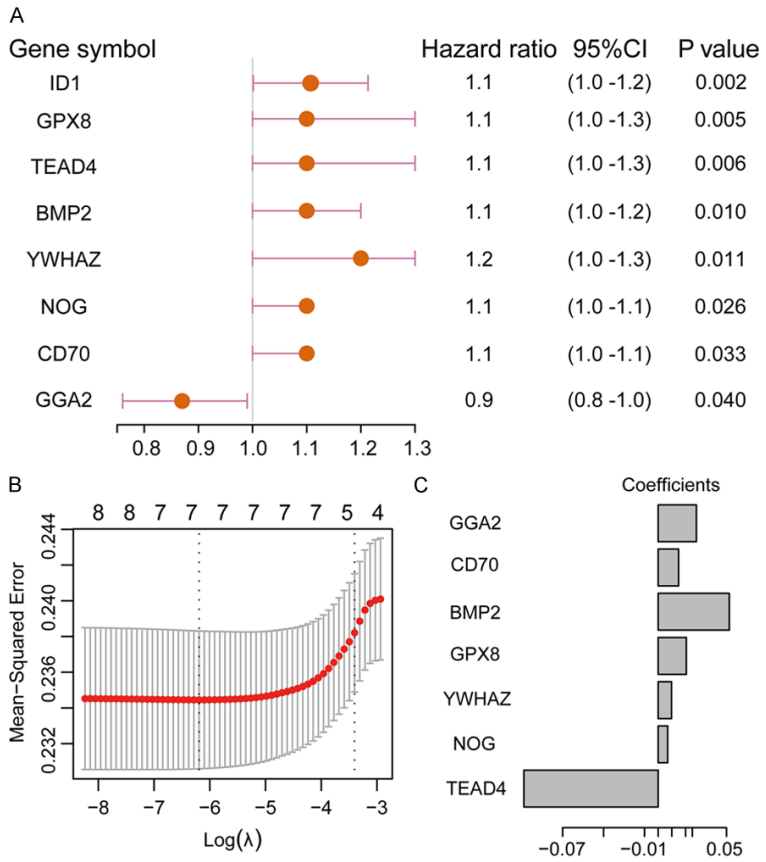

Figure 2. Construction of the prognostic gene signature. Forest plot of 8 genes (A). Distribution of lambda values for LASSO analysis (B). Coefficient statistics of 7 genes (C).

The study was conducted according to the guidelines of the Declaration of Helsinki and approved by the Biomedical Research Ethic Committee of Qilu Hospital of Shandong University (KYLL-2017KS-189). All patients had signed an informed consent form.

Results

Identification of m6A regulator-related genes and functional enrichment analysis

We observed differences in m6A regulators expression between tumor and normal samples (**Figure 1A**). Most of the writers and readers showed higher expression levels in the tumor samples. Previous studies had reported that increased m6A mRNA methylation promoted the progression of NSCLC [21, 22].

By Pearson's test, we detected 1809 genes that were significantly associated with m6A regulators in the terms of mutation, 34159 genes in the terms of gene expression, and 19296 genes in the terms of CNV. Next, we defined the intersection of these genes as the m6A regulator-related gene (**Figure 1B**).

We found 17 signaling pathways from enrichment analysis in KEGG based on the m6A regulator-related genes (**Figure 1C**). Pathway interaction network analysis showed that the IL-17 signaling pathway was in a central position (**Figure 1D**). In addition, regarding the GO analysis, these genes were found to be more associated with molecular binding, cell biological activities and signaling exchanges between cells (**Figure 1E**).

Establishment and validation of the prognostic gene signature

We performed univariate Cox regression analysis to screen for prognostic contributions in m6A regulator-related genes. And 8 genes were significant (**Figure 2A**). They were ID1, GPX8, TEAD4, BMP2, YWHAZ, NOG, CD70, and GGA2. Then, we successfully generated a prognostic gene signature by LASSO (**Figure 2B**, **2C**).

In the training cohort, the area under the curves (AUC) for the risk score were all greater than 0.55 (**Figure 3A**). Patients in the high-risk group had lower survival rates. In the validation cohorts, the risk score showed similarly good predictive ability to discriminate the patients (**Figure 3B**, **3C**). Analysis of the clinical characteristics of the training cohort revealed that patients with higher risk score exhibited lower survival rates among the age, stage M and stage T (Supplementary Figure 1). These data suggested a high predictive power and stability of the risk score.

Risk score and tumor microenvironment

As shown in **Figure 4A**, the mutational load that was observed in the high-risk group was higher

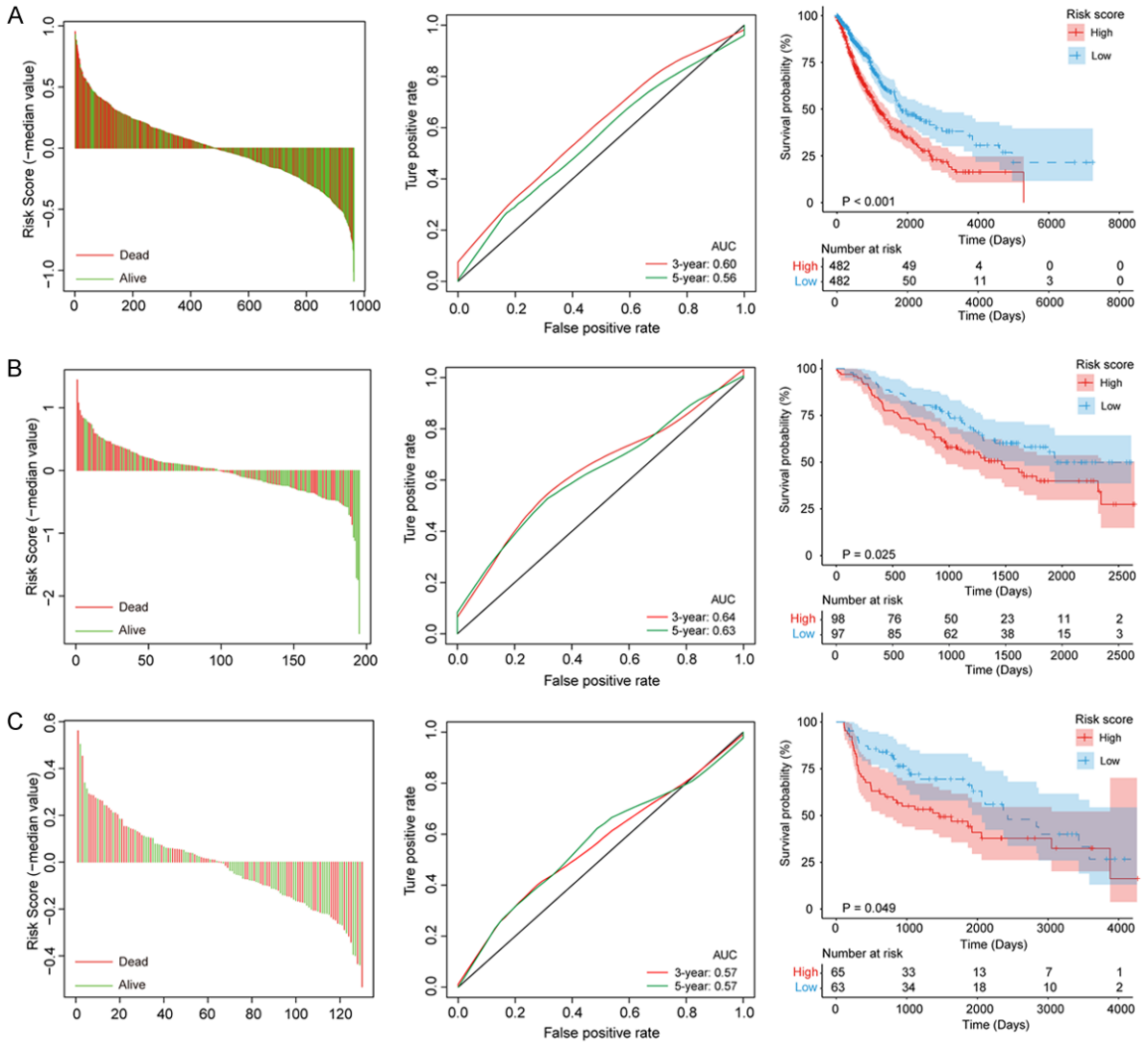

Figure 3. Validation of the prognostic gene signature. Risk score distribution, time-dependent ROC curves and KM survival analysis in TCGA (A), GSE81089 (B) and Raponi 2006 datasets (C).

than that in the low-risk group. But most mutated genes were shared between the two subgroups. In particular, the proportion of samples with mutations in the TP53 was greater in the high-risk group than in the low-risk group, and the same was observed for the TTN.

Correlation analysis showed a significant negative correlation between TMB and risk score (**Figure 4B**). And the infiltration levels of B cell, T cells regulatory and other immune cells were decreased with the increased risk score.

Finally, the data showed significant differences in response to immunotherapy between the high- and low-risk groups. A higher risk score observed for patients who did not exhibit response (**Figure 5A**). And patients with high risk scores had bad prognosis (**Figure 5B**). Additionally, we noticed that the proportion of immune nonresponsive samples was higher in the high-risk group than in the low-risk group (**Figure 5C**). The above results suggest that the risk score can be a marker of the immune response.

GGA2 inhibited NSCLC by downregulating METTL3

In Supplementary Figure 2, we found that the average expression of GGA2 was decreased in tumor compared with normal tissues (n = 6). Then, we successfully established GGA2-overexpressing cell lines (**Figure 6A**). As show

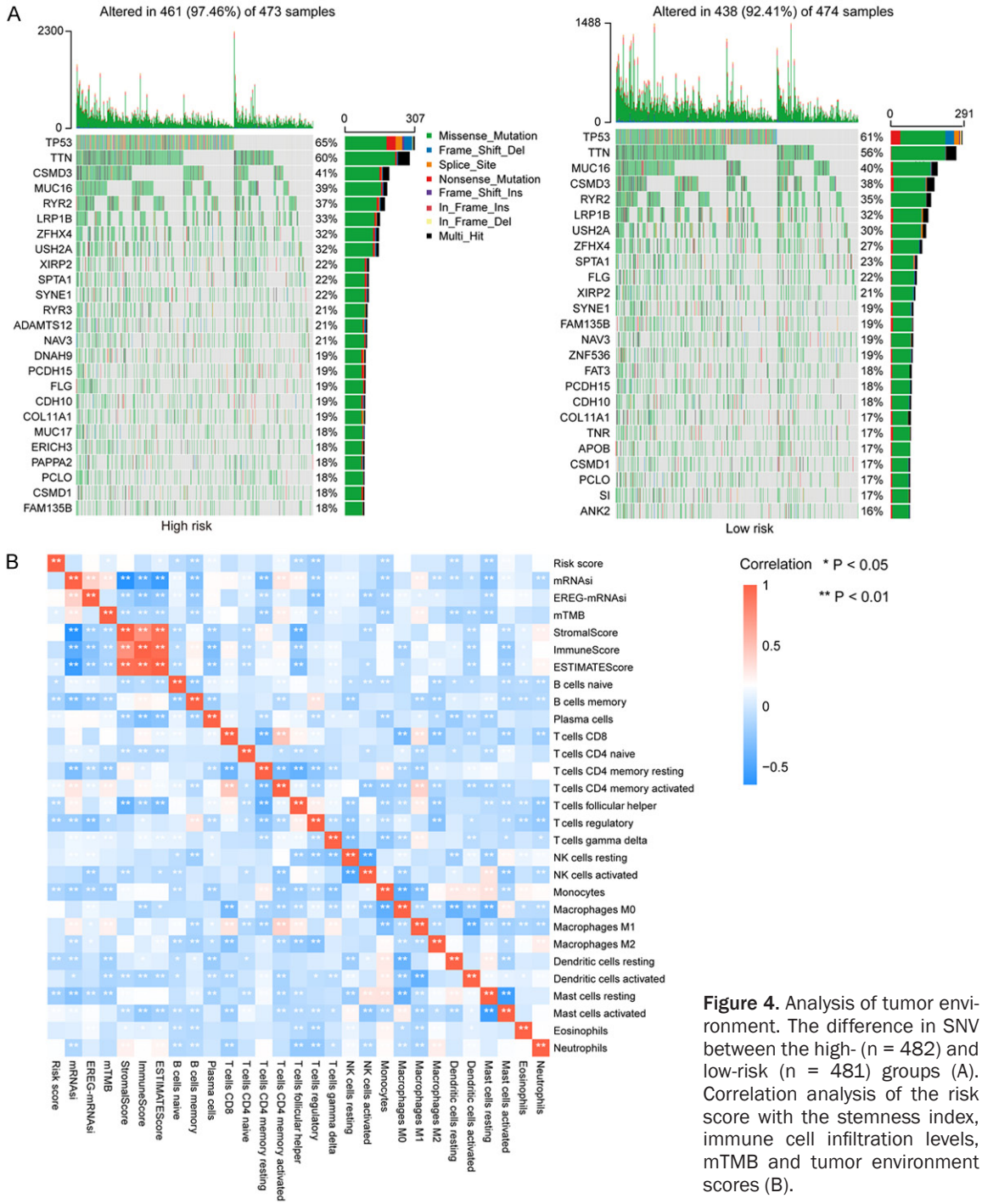

Figure 4. Analysis of tumor environment. The difference in SNV between the high- (n = 482) and low-risk (n = 481) groups (A). Correlation analysis of the risk score with the stemness index, immune cell infiltration levels, mTMB and tumor environment scores (B).

in **Figure 6B**, GGA2 inhibited cellular proliferation both in three cell lines. This phenomenon was further validated in EdU staining (**Figure 6C**). Moreover, the migration and invasion of NSCLC cells were also attenuated (**Figure 6D**). Next, we detected the m6A% content in total RNA. The data revealed that overexpression of GGA2 decreased m6A abundance in NSCLC cells compared to controls (**Figure 6E**). To further explore the role of GGA2 in m6A, we examined the protein level of readers and erasers. Western blot analysis indicated the METTL3 expression was downregulated. The expression of other readers and eraser was not statistically altered (**Figure 6F**).

The role of METTL3 in NSCLC was reported by Mengmeng Chen et al [23]. They found that

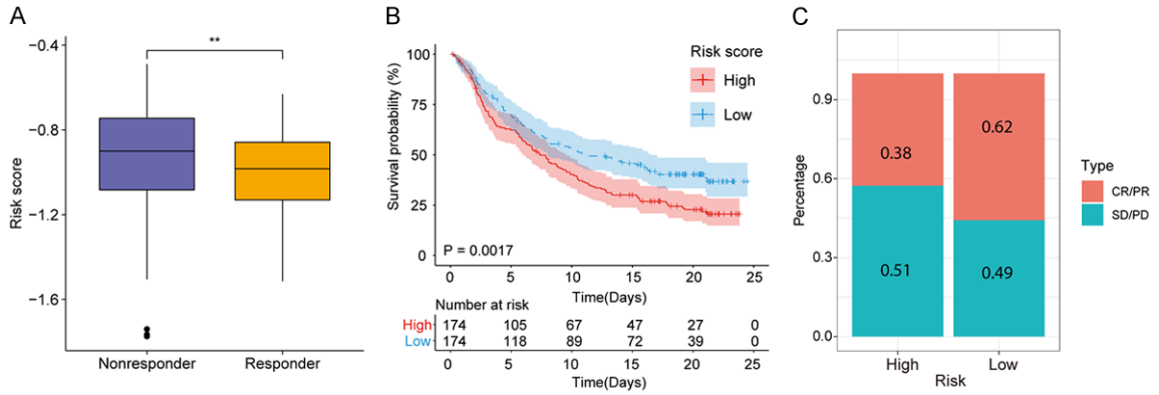

Figure 5. Risk score and immunotherapy response. Risk scores were higher in samples without immune response (**, P < 0.01) (A). Significant prognostic differences between the high- and low-risk groups (B). Higher proportion of non-response samples in the high-risk group than in the low-risk group (C).

knockdown of METTL3 significantly inhibited the proliferation and motility of NSCLC cells. Based on their work, we knocked down METTL3 in GGA2 overexpressing cells to further identify that GGA2 inhibited NSCLC cells via downregulating METTL3 (Supplementary Figure 3).

As shown in **Figure 7A**, the m6A content in total RNA was further decreased in co-treated (OE-GGA2+si-METTL3) NSCLC cells. And both cellular proliferation and motility were also further inhibited (**Figure 7B-D**). Together, these data indicated GGA2 inhibited cell proliferation and motility by decreasing m6A abundance via downregulating METTL3.

Discussion

Non-small cell lung cancer (NSCLC) is one of the leading causes of death in oncology patients worldwide and the most predominant type of lung cancer. The five-year survival rate of NSCLC is less than 15% due to its strong invasive and metastatic ability [24]. As the most common means of RNA modification in eukaryotes, m6A modifications are frequently involved in mRNA metabolism and translation, thus affecting protein expression levels. When regulators of m6A are mutated, with copy number variation and disturbed expression, the genes they modify are also disturbed and thus involved in the cancer process. However, the biological functions and key target genes of these m6A regulators in NSCLC remain unclear. In the present study, we used data from TCGA to identify genes associated with m6A regulators. Next, a prognostic signature was generated and validated based on the identified genes. The data showed that the signature could effectively be used to assess the prognosis of patients.

Abnormalities of the immune system profoundly affect tumor development. Therapies targeting the immune system have also revolutionized the treatment strategy for many malignancies, including NSCLC [25]. However, few studies have addressed the relationship between m6A regulator-related genes and immune infiltration in NSCLC. Therefore, we further explored the clinical value of the generated signature. We analyzed the correlation between immune infiltration and the signature. The data showed that the infiltration levels of multiple immune cells such as resting dendritic cells and resting mast cells were decreased in patient with high risk scores. These findings suggest that decreased immune infiltration levels may be a factor in the poorer prognosis of patients in the high-risk group. Our data also indicate that risk scores can be markers of immune response. Together, m6A regulator-related genes are closely associated with immune abnormalities in NSCLC.

In addition to immune abnormalities, we also focused on other possible mechanisms by which m6A regulator-related genes affect the prognosis of NSCLC. It has been suggested that the accumulation of genetic alterations leads to abnormal cell proliferation and eventually tumorigenesis [26, 27]. These genetic alterations are considered to be the drivers of

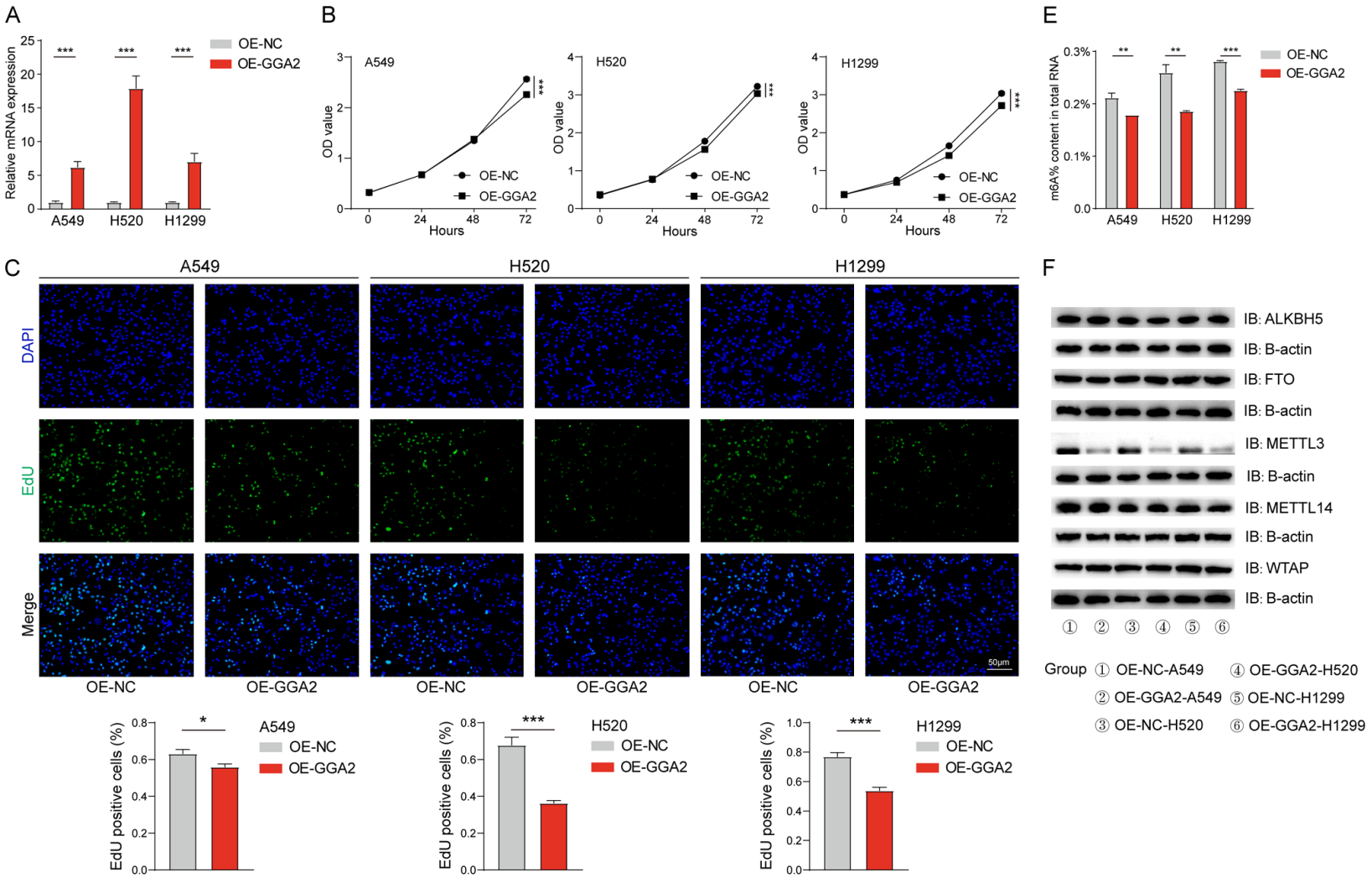
A
Relative mRNA expression
OE-NC
OE-GGA2
A549
H520
H1299
B
OD value
Hours
C
DAPI
EdU
Merge
50μm
EdU positive cells (%)
E
m6A% content in total RNA
F
IB: ALKBH5
IB: B-actin
IB: FTO
IB: METTL3
IB: METTL14
IB: WTAP
Group ① OE-NC-A549 ④ OE-GGA2-H520
② OE-GGA2-A549 ⑤ OE-NC-H1299
③ OE-NC-H520 ⑥ OE-GGA2-H1299

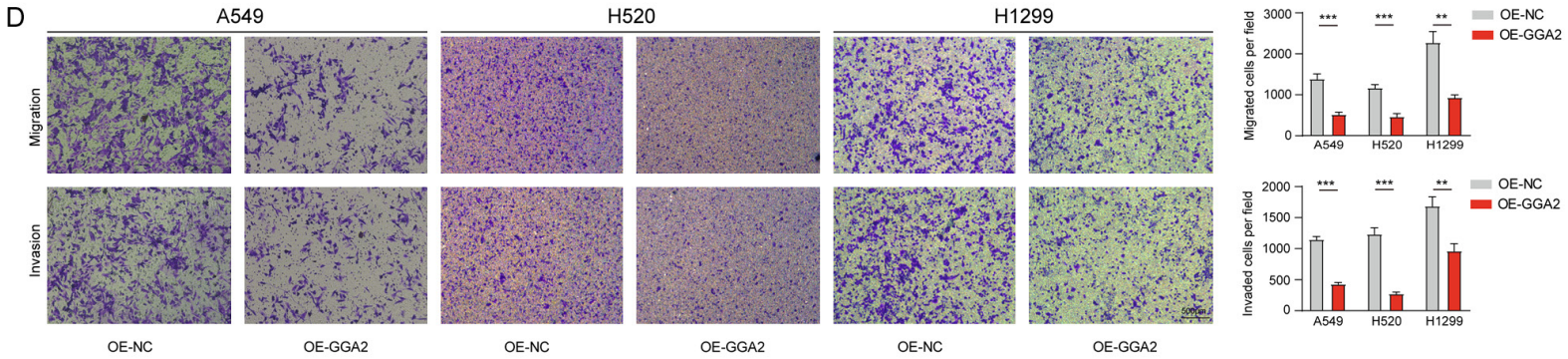

Figure 6. GGA2 inhibited NSCLC cells. Construction of NSCLC cell lines overexpressing GGA2, *P* value was calculated by 2-tailed Student t test (***, P < 0.001) (A). Cell proliferation was detected by measuring the optical density in 450 nm, *P* value was calculated by 2-tailed Student t test (***, P < 0.001) (B). EdU staining (green fluorescence) on cell proliferation 3 days after the construction of cell lines, nuclei were counterstained blue with DAPI (Scale bars, 50 μm) (*, P < 0.05; ***, P < 0.001) (C). Representative images of Transwell assays (migration and invasion) after 24 hours incubation (Scale bars, 500 μm) (***, P < 0.001) (D). Detection of m6A content in total RNA, *P* value was calculated by 2-tailed Student t test (**, P < 0.01; ***, P < 0.001) (E). The expression of m6A regulators were detected by western blot (F).

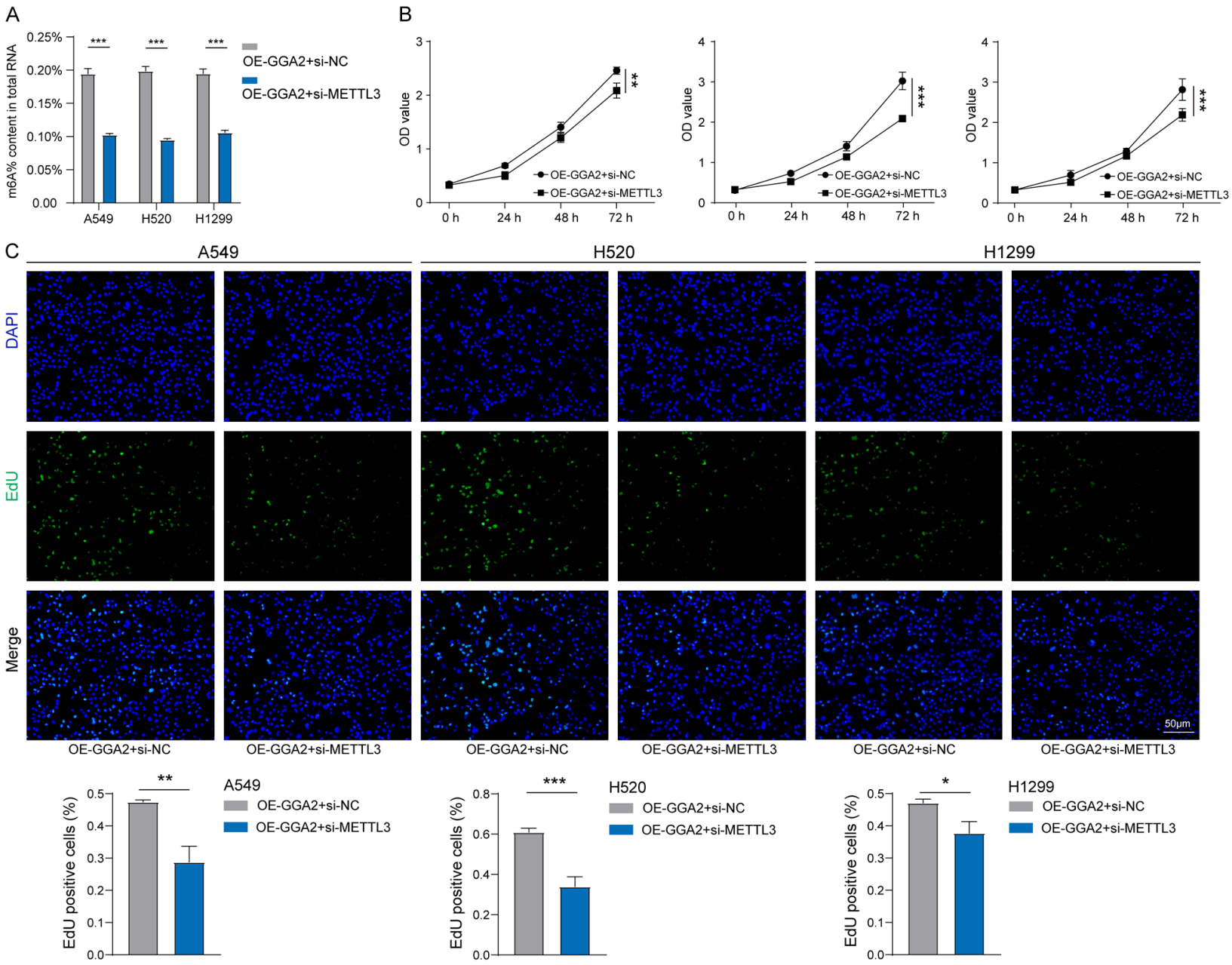
A
m6A% content in total RNA
0.25%
0.20%
0.15%
0.10%
0.05%
0.00
***
***
***
A549
H520
H1299
OE-GGA2+si-NC
OE-GGA2+si-METTL3
B
OD value
**
***
***
0 h
24 h
48 h
72 h
OE-GGA2+si-NC
OE-GGA2+si-METTL3
C
A549
H520
H1299
DAPI
EdU
Merge
50μm
OE-GGA2+si-NC
OE-GGA2+si-METTL3
EdU positive cells (%)
**
***
*
A549
H520
H1299

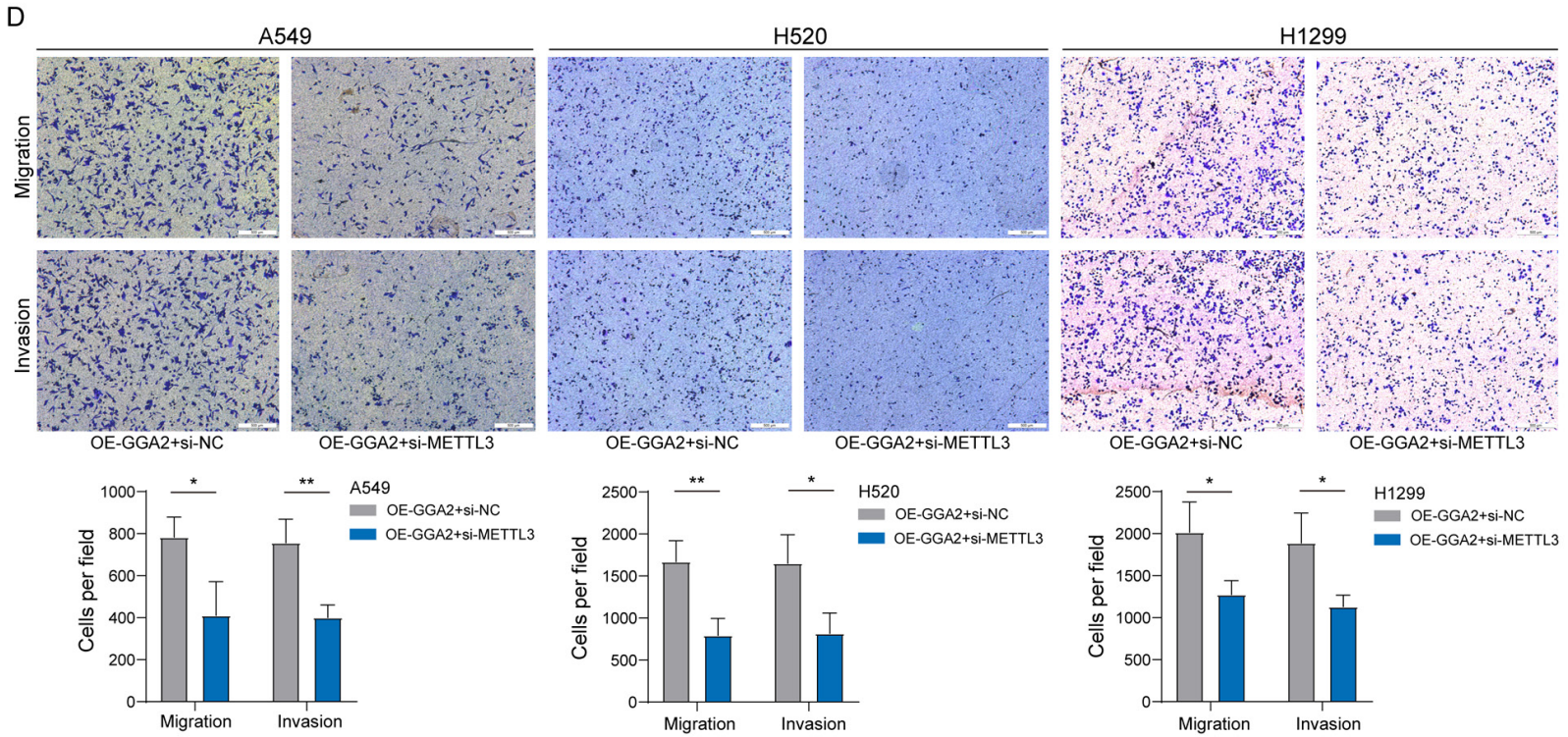

Figure 7. GGA2 inhibited NSCLC cells by downregulating METTL3. Detection of m6A content in total RNA, *P* value was calculated by 2-tailed Student t test (***, P < 0.001) (A). Cell proliferation was detected by measuring the optical density (OD) in 450 nm, *P* value was calculated by 2-tailed Student t test (**, P < 0.01; ***, P < 0.001) (B). EdU staining (green fluorescence) on cell proliferation 3 days after the construction of cell lines, nuclei were counterstained blue with DAPI (Scale bars, 50 μm) (*, P < 0.05; **, P < 0.01; ***, P < 0.001) (C). Representative images of Transwell assays (migration and invasion) after 24 hours incubation (Scale bars, 500 μm) (*, P < 0.05; **, P < 0.01) (D).

tumors. Therefore, genetic mutations are very important for tumorigenesis and tumor development [28]. After analyzing the mutation profile in NSCLC, we found a significantly higher proportion of TP53 and TTN mutations in the high-risk groups than in the low-risk groups. Both TP53 and TTN are now known to be driver genes of tumors. This finding may be associated with the higher mortality observed in the high-risk group.

In our study, the role of GGA2 in NSCLC was explored. GGA2 encodes a member of the Golgi-localized, gamma adaptin ear-containing, ARF-binding family, which regulate the trafficking of proteins. Some relationships between GGA2 and lung cancer had been found in previous researches. Rs2285521 in GGA2 contributed to lung cancer susceptibility in European populations [29]. Our data showed that overexpressed GGA2 suppressed lung cancer by decreasing the expression level of METTL3. It has been reported that METTL3 promoted the translation of EGFR [30]. The driving effect of EGFR on NSCLC had also been demonstrated [31]. Therefore, we believe that the inhibitory effect of GGA2 on NSCLC is likely to be ultimately achieved through the inhibition of EGFR.

However, there are some limitations to this study. The interaction between m6A regulators and prognostic genes needs to be further validated experimentally to better explain our findings. In addition, although the signature we generated has been validated in two external cohorts, an independent cohort consisting of more NSCLC patients is needed to further validate the model prospectively.

Conclusions

In conclusion, our work provides insights into the function of m6A regulator-related genes and offers evidence for predicting the immune response in NSCLC patients. In this study, we analyzed the genes related to m6A regulators in NSCLC from the perspective of m6A gene expression and genomic variation. The potential application of these genes as predictive biomarkers of immunotherapeutic response was highlighted.

Acknowledgements

This research was supported by the National Natural Science Foundation of China (81-702261) and the Natural Science Foundation of Shandong Province (ZR202111140152, ZR2021MH293).

Disclosure of conflict of interest

None.

Address correspondence to: Hongxin Cao, Department of Medical Oncology, Qilu Hospital of Shandong University, No. 107, Wenhuaxi Road, Lixia District, Jinan 250000, Shandong, China. E-mail: caohongxin@sdu.edu.cn

References

[1] Desrosiers R, Friderici K and Rottman F. Identification of methylated nucleosides in messenger RNA from Novikoff hepatoma cells. Proc Natl Acad Sci U S A 1974; 71: 3971-3975.

[2] Molinie B and Giallourakis CC. Genome-wide location analyses of N6-methyladenosine modifications (m(6)A-Seq). Methods Mol Biol 2017; 1562: 45-53.

[3] Nguyen S, Meletis K, Fu D, Jhaveri S and Jaenisch R. Ablation of de novo DNA methyltransferase Dnmt3a in the nervous system leads to neuromuscular defects and shortened lifespan. Dev Dyn 2007; 236: 1663-1676.

[4] Harper JE, Miceli SM, Roberts RJ and Manley JL. Sequence specificity of the human mRNA N6-adenosine methylase in vitro. Nucleic Acids Res 1990; 18: 5735-5741.

[5] Liu J, Yue Y, Han D, Wang X, Fu Y, Zhang L, Jia G, Yu M, Lu Z, Deng X, Dai Q, Chen W and He C. A METTL3-METTL14 complex mediates mammalian nuclear RNA N6-adenosine methylation. Nat Chem Biol 2014; 10: 93-95.

[6] Zhao BS, Roundtree IA and He C. Post-transcriptional gene regulation by mRNA modifications. Nat Rev Mol Cell Biol 2017; 18: 31-42.

[7] Li XC, Jin F, Wang BY, Yin XJ, Hong W and Tian FJ. The m6A demethylase ALKBH5 controls trophoblast invasion at the maternal-fetal interface by regulating the stability of mRNA. Theranostics 2019; 9: 3853-3865.

[8] Meyer KD, Saletore Y, Zumbo P, Elemento O, Mason CE and Jaffrey SR. Comprehensive analysis of mRNA methylation reveals enrichment in 3' UTRs and near stop codons. Cell 2012; 149: 1635-1646.

[9] Alarcón CR, Goodarzi H, Lee H, Liu X, Tavazoie S and Tavazoie SF. HNRNPA2B1 is a mediator of m(6)A-dependent nuclear RNA processing events. Cell 2015; 162: 1299-1308.

[10] Horiuchi K, Kawamura T, Iwanari H, Ohashi R, Naito M, Kodama T and Hamakubo T. Identification of Wilms' tumor 1-associating protein complex and its role in alternative splicing and

the cell cycle. J Biol Chem 2013; 288: 33292-33302.
[11] Ben-Haim MS, Moshitch-Moshkovitz S and Rechavi G. FTO: linking m6A demethylation to adipogenesis. Cell Res 2015; 25: 3-4.
[12] Liu N, Dai Q, Zheng G, He C, Parisien M and Pan T. N(6)-methyladenosine-dependent RNA structural switches regulate RNA-protein interactions. Nature 2015; 518: 560-564.
[13] Dominissini D, Moshitch-Moshkovitz S, Schwartz S, Salmon-Divon M, Ungar L, Osenberg S, Cesarkas K, Jacob-Hirsch J, Amariglio N, Kupiec M, Sorek R and Rechavi G. Topology of the human and mouse m6A RNA methylomes revealed by m6A-seq. Nature 2012; 485: 201-206.
[14] Zhang C, Samanta D, Lu H, Bullen JW, Zhang H, Chen I, He X and Semenza GL. Hypoxia induces the breast cancer stem cell phenotype by HIF-dependent and ALKBH5-mediated m6A-demethylation of NANOG mRNA. Proc Natl Acad Sci U S A 2016; 113: E2047-E2056.
[15] Zhang S, Zhao BS, Zhou A, Lin K, Zheng S, Lu Z, Chen Y, Sulman EP, Xie K, Bögler O, Majumder S, He C and Huang S. m6A demethylase ALKBH5 maintains tumorigenicity of glioblastoma stem-like cells by sustaining FOXM1 expression and cell proliferation program. Cancer Cell 2017; 31: 591-606, e6
[16] Wang S, Sun C, Li J, Zhang E, Ma Z, Xu W, Li H, Qiu M, Xu Y, Xia W, Xu L and Yin R. Roles of RNA methylation by means of N6-methyladenosine (m6A) in human cancers. Cancer Lett 2017; 408: 112-120.
[17] Zhang B, Wu Q, Li B, Wang D, Wang L and Zhou YL. m6A regulator-mediated methylation modification patterns and tumor microenvironment infiltration characterization in gastric cancer. Mol Cancer 2020; 19: 53.
[18] You Y, Ma W, Wang F, Jiao G, Zhang L, Zhou H, Wu W, Wang H and Chen Y. Ortho-silicic acid enhances osteogenesis of osteoblasts through the upregulation of miR-130b which directly targets PTEN. Life Sci 2021; 264: 118680.
[19] Li X, Dai Z, Liu J, Sun Z, Li N, Jiao G and Cao H. Characterization of the functional effects of ferredoxin 1 as a cuproptosis biomarker in cancer. Front Genet 2022; 13: 969856.
[20] Zheng D, Xia K, Yu L, Gong C, Shi Y, Li W, Qiu Y, Yang J and Guo W. A novel six metastasis-related prognostic gene signature for patients with osteosarcoma. Front Cell Dev Biol 2021; 9: 699212.
[21] Jin D, Guo J, Wu Y, Du J, Yang L, Wang X, Di W, Hu B, An J, Kong L, Pan L and Su G. m(6)A mRNA methylation initiated by METTL3 directly promotes YAP translation and increases YAP activity by regulating the MALAT1-miR-1914-3p-YAP axis to induce NSCLC drug resistance and metastasis. J Hematol Oncol 2019; 12: 135.
[22] Yin H, Chen L, Piao S, Wang Y, Li Z, Lin Y, Tang X, Zhang H, Zhang H and Wang X. m6A RNA methylation-mediated RMRP stability renders proliferation and progression of non-small cell lung cancer through regulating TGFBR1/SMAD2/SMAD3 pathway. Cell Death Differ 2023; 30: 605-617.
[23] Chen M, Zhang Q, Zheng S, Guo X, Cao L, Ren Y, Qian Y, Wang M, Wu X and Xu K. Cancer-associated fibroblasts promote migration and invasion of non-small cell lung cancer cells via METTL3-mediated RAC3 m(6)A modification. Int J Biol Sci 2023; 19: 1616-1632.
[24] Bray F, Ferlay J, Soerjomataram I, Siegel RL, Torre LA and Jemal A. Global cancer statistics 2018: GLOBOCAN estimates of incidence and mortality worldwide for 36 cancers in 185 countries. CA Cancer J Clin 2018; 68: 394-424.
[25] Naidoo J, Nishino M, Patel SP, Shankar B, Rekhtman N, Illei P and Camus P. Immune-related pneumonitis after chemoradiotherapy and subsequent immune checkpoint blockade in unresectable stage III non-small-cell lung cancer. Clin Lung Cancer 2020; 21: e435-e444.
[26] Hanahan D and Weinberg RA. The hallmarks of cancer. Cell 2000; 100: 57-70.
[27] Stratton MR, Campbell PJ and Futreal PA. The cancer genome. Nature 2009; 458: 719-724.
[28] Yates LR and Campbell PJ. Evolution of the cancer genome. Nat Rev Genet 2012; 13: 795-806.
[29] Yang W, Liu H, Zhang R, Freedman JA, Han Y, Hung RJ, Brhane Y, McLaughlin J, Brennan P, Bickeboeller H, Rosenberger A, Houlston RS, Caporaso NE, Landi MT, Brueske I, Risch A, Christiani DC, Amos CI, Chen X, Patierno SR and Wei Q. Deciphering associations between three RNA splicing-related genetic variants and lung cancer risk. NPJ Precis Oncol 2022; 6: 48.
[30] Lin S, Choe J, Du P, Triboulet R and Gregory RI. The m(6)A methyltransferase METTL3 promotes translation in human cancer cells. Mol Cell 2016; 62: 335-345.
[31] Harrison PT, Vyse S and Huang PH. Rare epidermal growth factor receptor (EGFR) mutations in non-small cell lung cancer. Semin Cancer Biol 2020; 61: 167-179.

Supplementary Table 1. Primers used in the study

Gene symbol	Full name		Sequence (5'-3')
GGA2	Gamma-Adaptin-Related Protein 2	Forward	AATCAATGCCCCAGTCACCT
		Reverse	CTTCTTTGGGACACTTGCTGC
METTL3	Methyltransferase 3	Forward	CAAGGAGGAGTGCATGAAAG
		Reverse	GGCTTGGCGTGTGGTCTTTG
β-actin	Actin Beta	Forward	CTCCATCCTGGCCTCGCTGT
		Reverse	GCTGTCACCTTCACCGTTCC

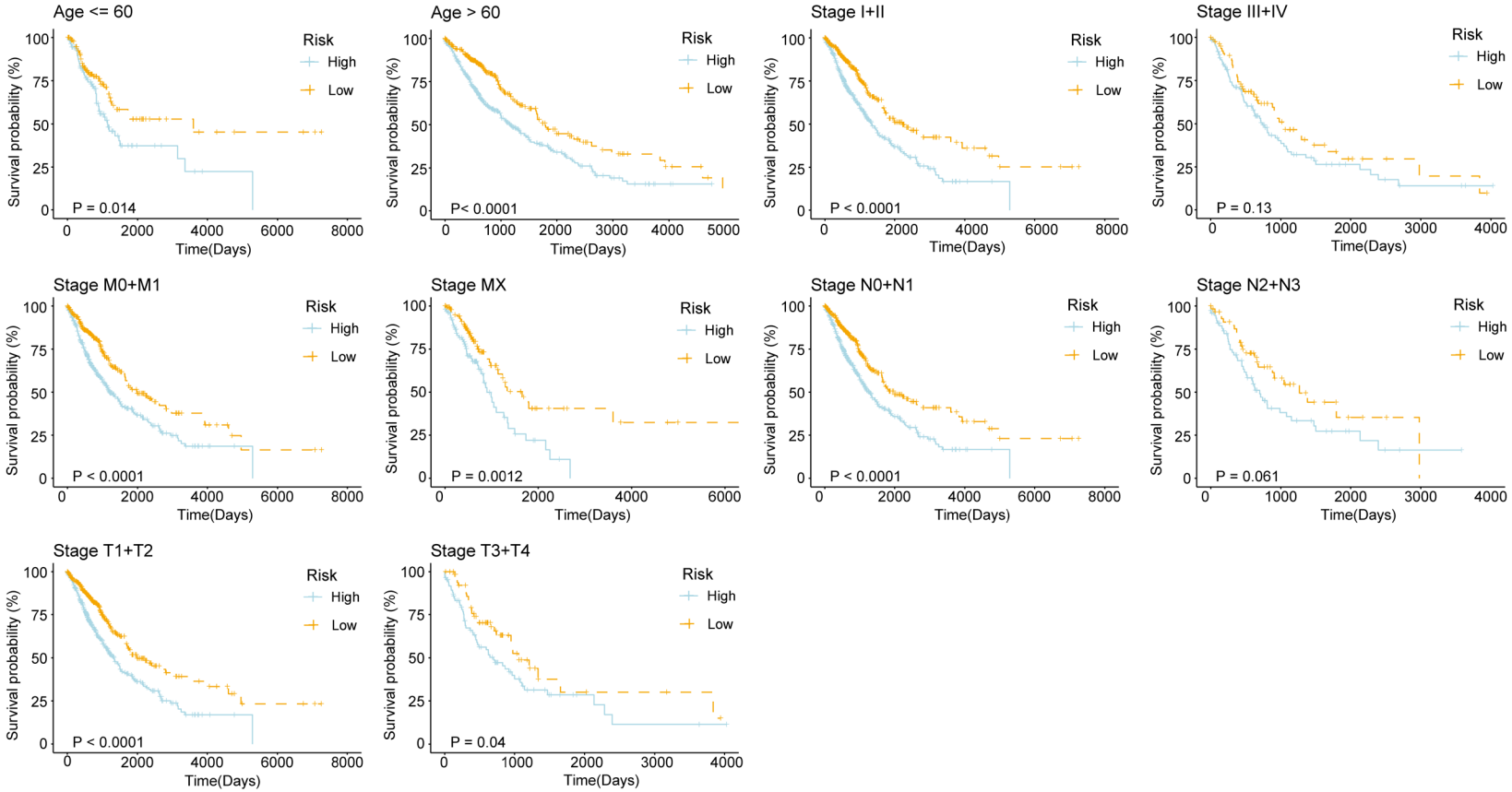

Supplementary Figure 1. Validity and stability assessment of the gene signature.

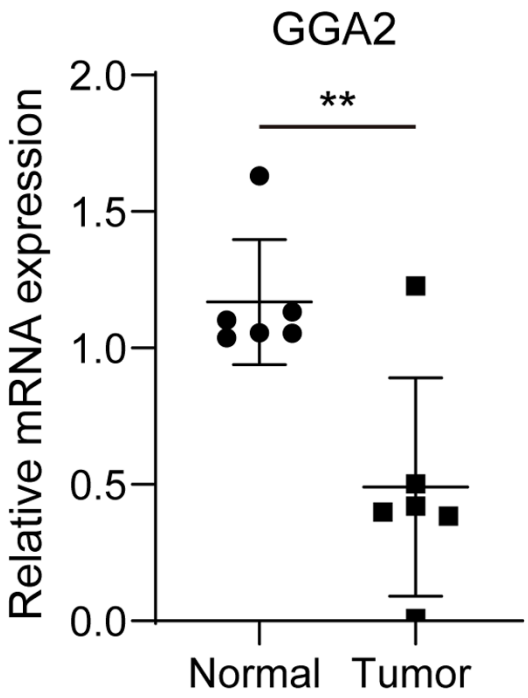

Supplementary Figure 2. The mRNA expression of GGA2 in tumor and normal samples.

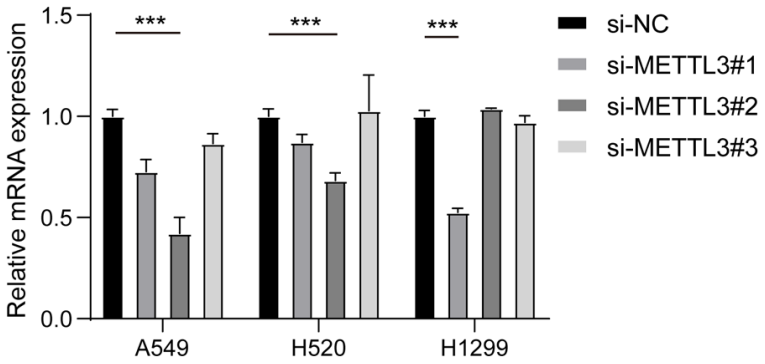

Supplementary Figure 3. Construction of cell lines.